Article

Advances in Structural Engineering

Advances in Structural Engineering
2016, Vol. 19(6) 953–965

DOI: 10.1177/1369433216630461
ase.sagepub.com
SAGE

Study of vertical bending vibration behavior of continuous prestressed concrete box girders with corrugated steel webs

Wei Ji[1,2], Lu Deng[1], Shizhong Liu[2] and Pengzhen Lin[2]

Abstract

Prestressed concrete girders with corrugated steel webs have received considerable attention in the past two decades due to their light self-weight and high prestressing efficiency. Most previous studies were focused on the static behavior of corrugated steel webs and simple beams with corrugated steel webs. The natural frequencies are very important characteristics when evaluating the dynamic responses of a bridge under external loads; however, very few studies have been conducted to investigate the dynamic behavior of full prestressed concrete girders or bridges with corrugated steel webs, and no simple formulas are available for estimating the natural frequencies of prestressed concrete girder bridges with corrugated steel webs. In addition, experimental work on full-scale bridges or scale bridge models is very limited. In this article, formulas for predicting the vertical bending vibration frequencies of prestressed concrete box girders with corrugated steel webs are proposed based on Hamilton's energy variational principle. A one-tenth scale model is developed for an existing prestressed concrete box-girder bridge with corrugated steel webs. The frequencies predicted by the proposed formulas are compared to the finite element analysis results and also the experimental results from the scale bridge model. Good agreement is achieved between these results, indicating that the proposed formulas can provide a reliable and efficient tool to predict the vertical bending vibration frequencies of prestressed concrete box-girder bridges with corrugated steel webs.

Keywords

corrugated steel web, energy variational principle, prestressed concrete box girder, scale bridge model, vibration frequency

Introduction

In the past two decades, prestressed concrete (PC) girders with corrugated steel webs (CSWs) have provided an excellent alternative to conventional concrete girder bridges. This new type of PC girder bridges with CSWs is designed to take full advantages of the material properties of the concrete flanges, prestressed tendons, and steel webs. As shown in Figure 1 (Ji et al., 2012), the concrete flanges provide the required bending capacity, while the CSWs provide the desired shear capacity but have little contribution to the bending capacity.

However, the idea of replacing the concrete webs in conventional PC box girders with CSWs can not only substantially reduce the dead load of the girder but also speed up the construction process and therefore reduce the total construction cost. Moreover, the CSWs do not absorb much prestressing force in the concrete flanges and can thus achieve higher prestressing efficiency than conventional PC box girders. The Maupré Bridge in France (Hassanein and Kharoob, 2014) and the Caochanggou Bridge in China, shown in Figure 2, are two examples of bridge structures adopting such girders.

Most of previous studies focused on the shear buckling of CSWs (Driver et al., 2006; Easley and McFarland, 1969; Elgaaly et al., 1996; Moon et al., 2009; Yi et al., 2008) because the CSWs usually fail due to shear buckling or yielding. The flexural behavior of I-girders with CSWs has also been studied by many researchers (Abbas et al., 2007a, 2007b; Elgaaly et al., 1997; Nguyen et al., 2010; Sayed-Ahmed, 2005). In addition, the fatigue performance of girders with CSWs was also studied by Ibrahim (2001). Besides, the

[1]College of Civil Engineering, Hunan University, Changsha, China
[2]College of Civil Engineering, Lanzhou Jiaotong University, Lanzhou, China

Corresponding author:
Lu Deng, College of Civil Engineering, Hunan University, Changsha, Hunan 410082, China.
Email: denglu@hnu.edu.cn

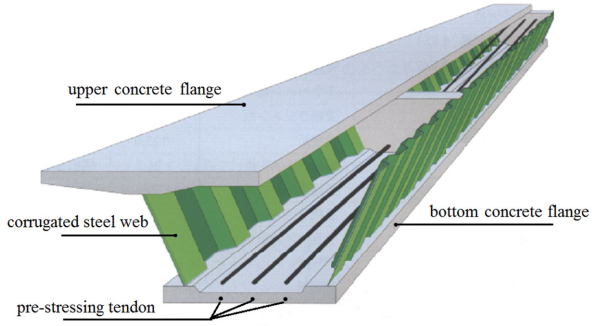

Figure 1. Main components of a PC box girder with corrugated steel webs (Ji et al., 2012).

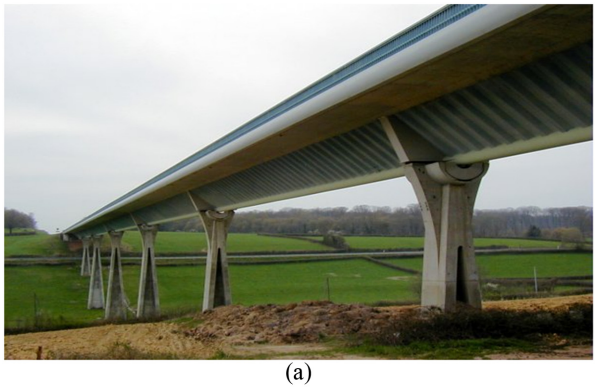

(a)

(b)

Figure 2. Concrete bridge girders with CSWs: (a) Maupré Bridge and (b) Caochanggou Bridge.

accordion effect of steel beams with CSWs was studied by Huang et al. (2004). Researchers also studied the orthotropic properties of corrugated webs and proposed equivalent orthotropic plate models (Bertagnoli et al., 2012). However, very few studies provided experimental verification of these orthotropic plate models.

However, most previous studies were focused on the behavior of CSWs or steel beams with CSWs rather than the performance of a full PC girder or a full bridge with CSWs, and very few experimental studies have been reported on the performance of PC girders with CSWs (Mo et al., 2000, 2003). In addition, the dynamic behavior of PC girders with CSWs received much less attention than the static behavior.

The dynamic characteristics of a bridge in terms of its vibration frequencies and mode shapes are very important when evaluating the dynamic performance of a bridge under external loads. For instance, the previous Ontario bridge design code (Ontario Ministry of Transportation and Communications (OMTC), 1983) and the current Chinese bridge design code (Ministry of Communication of the People's Republic of China (MCPRC), 2004) both defined the dynamic impact factor as a function of the fundamental frequency of bridges. In practice, it is also important to have a good estimation of the fundamental frequency of a bridge to be constructed in order to avoid the possible resonance with heavy trucks which usually have a quite narrow range of frequencies between 1.5 and 4.5 Hz (Moghimi and Ronagh, 2008).

The main purpose of this article is to study the vertical bending vibration frequencies of continuous PC girders with CSWs. The governing differential equations of motion for the free vibration of continuous PC girders with CSWs are derived using Hamilton's energy variational principle. Formulas for predicting the vertical bending vibration frequencies of PC box girders with CSWs are developed. The accuracy of the proposed formulas is verified against the experimental results on a scale bridge model and also the finite element (FE) analysis results. The results predicted by the proposed formulas are also compared to the results calculated using the Chinese bridge design code and existing research results.

Shear modulus of CSWs

The shear modulus of the CSWs used in this study is proposed by Samanta and Mukhopadhyay (1999) and is defined as

$$G_s = \frac{(L_1 + L_2)}{(L_1 + L_3)} \frac{E_s}{2(1 + v_s)} = \alpha G \qquad (1)$$

where G, E_s, and v_s are the shear modulus, Young's modulus of elasticity, and Poisson's ratio of the flat steel plates, respectively; α is the length reduction factor, which is the ratio of the projected length $(L_1 + L_2)$ to the actual length of the corrugated plates $(L_1 + L_3)$ shown in Figure 3. Since the value of α is less than 1, the shear modulus of CSWs is smaller than that of flat steel plates.

In order to investigate the effect of corrugation shape on the vertical bending vibration frequencies of

Table 1. Dimensions of corrugated steel webs.

Type of corrugation	L_1 (mm)	L_2 (mm)	L_3 (mm)	Length reduction factor, α
CW1	340	160	226	0.8834
CW2	330	270	330	0.9091
CW3	430	370	430	0.9302

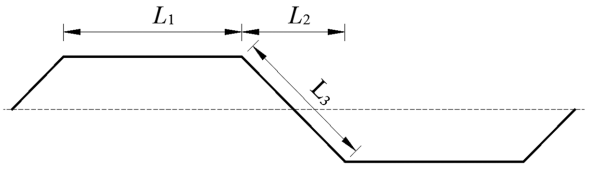

Figure 3. Corrugation configuration and geometric notation.

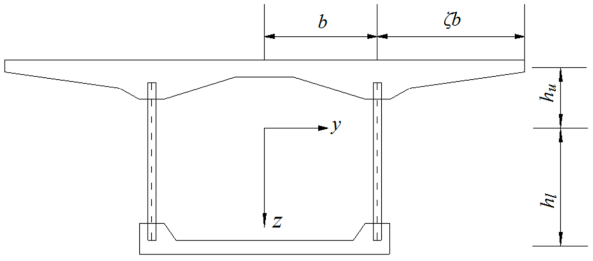

Figure 4. Cross-section of the box girder with CSWs.

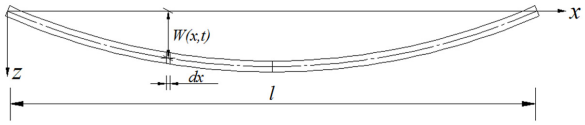

Figure 5. The vertical deformation of a simply supported girder under free vibration.

continuous PC girders with CSWs, three types of corrugation shape, namely CW1, CW2, and CW3, respectively, are considered. The dimensions of the three corrugation shapes are shown in Table 1. These are most common dimensions used for the PC box girders with CSWs in China and Japan.

Governing equations based on Hamilton's energy variational principle

Description of the problem and assumptions

The basic assumptions made for the PC box girders with CSWs investigated in this study are summarized as follows:

1. The flexural strength of the PC box girders with CSWs is solely provided by the concrete flanges while the CSWs have no contribution due to the accordion effect.
2. The materials of the girder are linear elastic, and the girder deflection and rotation are small.
3. The plane section assumption is adopted to calculate the stresses in the web of the box girder.
4. The geometry of the girder and the support conditions are symmetric. Also, the normal stress and displacement in the lateral direction are assumed to be zero.

Figure 4 shows a typical cross-section of the box girder with CSWs. Assuming that a simply supported PC box girder with CSWs is in a state of free vibration, as shown in Figure 5, the longitudinal displacement of the flanges can be described by a cubic-parabolic distribution, which is the modification of the conic-parabola proposed by Reissner (1946). Therefore, the longitudinal displacement of the box girder shown in Figure 5 at any point and any time can be expressed as follows (Luo et al., 2004)

$$W = W(x,t) \tag{2}$$

$$U(x,y,z,t) = -z\varphi(x,t) - z\omega_s(y)\xi(x,t) \tag{3}$$

where W is the vertical displacement of the box girder, $U(x,y,z,t)$ is the longitudinal displacement of the girder, $\varphi(x,t)$ is the angular rotation of the cross-section about the y-axis, $\xi(x,t)$ is the additional maximum angular rotation of the flange sections of the box girder about the y-axis due to the shear-lag effect, and $\omega_s(y)$ is the non-uniform distribution function of the shear-lag-induced longitudinal displacement along the flange width, which can be expressed by a cubic parabola as follows (Wu et al., 2003)

$$\omega_s(y) = \begin{cases} 1 - \frac{|y|^3}{b^3} & 0 \le |y| \le b \\ 1 - \frac{(b+\zeta b-|y|)^3}{(\zeta b)^3} & b \le |y| \le b + \zeta b \end{cases} \tag{4}$$

From equation (3), it can be seen that the cross-sections of the box girder no longer remain planar because of the shear-lag-induced warp displacement $\omega_s(y)$.

Considering the symmetry of shear strain, the normal strain and shear strain in the top and bottom flanges ($z = -h_u$, $z = h_l$) are given, respectively, by

$$\varepsilon_x = \frac{\partial U(x,y,z,t)}{\partial x} = -z[\varphi'(x,t) + \omega_s(y)\xi'(x,t)] \quad (5)$$

$$\gamma_{xy} = \frac{U(x,y,z,t)}{\partial y} = \left|-z\frac{d\omega_s(y)}{dy}\right|\xi'(x,t) \quad (6)$$

For the CSWs, the shear strain γ_{xz} can be expressed as

$$\gamma_{xz} = W'(x,t) - \varphi(x,t) \quad (7)$$

The vertical strain ε_z, transverse strain ε_y, and shear strain γ_{yz} are very small compared to the three terms in equations (5)–(7) and can therefore be neglected.

Governing differential equations

For the top flange, the strain energy can be calculated as follows

$$\bar{V}_u = \frac{1}{2}I_{su} \int_0^l \left\{E_c[\varphi'(x,t)]^2 + \frac{3}{2}E_c\varphi'(x,t)\xi'(x,t) + E_c\frac{9}{14}[\xi'(x,t)]^2 + \frac{9G_c\xi^2(x,t)}{5b^2}\right\}dx \quad (8)$$

where E_c and G_c are Young's modulus and shear modulus of the concrete flange, respectively; I_{su} is the moment of inertia of the top flange; and l is the span length of the girder.

For the bottom flange, the strain energy can be calculated as follows

$$\bar{V}_l = \frac{1}{2}I_{sl} \int_0^l \left\{E_c[\varphi'(x,t)]^2 + \frac{3}{2}E_c\varphi'(x,t)\xi'(x,t) + E_c\frac{9}{14}[\xi'(x,t)]^2 + \frac{9G_c\xi^2(x,t)}{5b^2}\right\}dx \quad (9)$$

where I_{sl} is the moment of inertia of the bottom flange.

The strain energy in the CSWs is

$$\bar{V}_f = \int_0^l \frac{G_sA_s}{2}\gamma_{xz}^2 dx \quad (10)$$

where A_s is the total cross-section area of two CSWs.

Thus, the internal potential energy of the PC box girder with CSWs is the sum of the strain energy in the concrete flanges and steel webs and can be calculated as

$$V = \bar{V}_u + \bar{V}_l + \bar{V}_f \quad (11)$$

The kinetic energy of a PC box girder with CSWs can be calculated as

$$T = \frac{1}{2}\int_0^l (\rho_cA_c + \rho_sA_s)\left(\frac{\partial W}{\partial t}\right)dx \quad (12)$$

where ρ_c and ρ_s are the densities of the concrete flanges and steel webs, respectively; A_c is the total cross-section area of the top flange and bottom flange.

The equations of motion and the boundary/continuity conditions are rigorously derived via Hamilton's energy variational principle, which requires

$$\delta\int_{t_1}^{t_2}(T-V)dt = \int_{t_1}^{t_2}(\delta T - \delta V)dt = 0 \quad (13)$$

According to equation (13), the governing differential equations and natural boundary conditions of the system are as follows

$$E_cI\varphi''(x,t) + \frac{3}{4}E_cI\xi''(x,t) + G_sA_s[W'(x,t) - \varphi(x,t)] = 0 \quad (14)$$

$$G_sA_s[W''(x,t) - \varphi'(x,t)] - (\rho_cA_c + \rho_sA_s)\ddot{W}(x,t) = 0 \quad (15)$$

$$E_cI\left[\frac{9G_c}{5E_cb^2}\xi(x,t) - \frac{9}{14}\xi''(x,t) - \frac{3}{4}\varphi''(x,t)\right] = 0 \quad (16)$$

$$\left[E_cI\varphi'(x,t) + \frac{3}{4}E_cI\xi'(x,t)\right]\delta\varphi\Big|_0^l = 0 \quad (17)$$

$$\left[\frac{3}{4}E_cI\varphi'(x,t) + \frac{9}{14}E_cI\xi'(x,t)\right]\delta\xi\Big|_0^l = 0 \quad (18)$$

$$G_sA_s[W'(x,t) - \varphi(x,t)]\delta W\Big|_0^l = 0 \quad (19)$$

Free vibration

The terms $W(x,t)$, $\varphi(x,t)$, and $\xi(x,t)$ in equations (2) and (3) can be easily rewritten in the following forms

$$W(x,t) = W(x)\sin(\omega t + \phi) \quad (20)$$

$$\xi(x,t) = \xi(x)\sin(\omega t + \phi) \quad (21)$$

$$\varphi(x,t) = \varphi(x)\sin(\omega t + \phi) \quad (22)$$

where ω is the circular frequency; ϕ is the initial phase angle.

After substituting equations (20)–(22) into equation (14) and combining equations (15) and (16), the governing differential equation for the free vibration of the

PC box girder with CSWs can be rewritten in terms of the vertical displacement $W(x,t)$ as shown below

$$W^{(6)}(x,t) + \left(\frac{\bar{m}\omega^2}{G_sA_s} - \frac{112G_c}{5E_cb^2}\right)W^{(4)}(x,t) - \left(\frac{8\bar{m}\omega^2}{E_cI} + \frac{112\bar{m}\omega^2G_c}{5G_sA_sE_cb^2}\right)W^{(2)}(x,t) + \frac{112\bar{m}\omega^2G_c}{5E_c^2b^2I}W(x,t) = 0 \quad (23)$$

where $\bar{m} = \rho_cA_c + \rho_sA_s$.

If equation (23) has non-zero solutions, then the term $\sin(\omega t + \phi)$ is not always equal to zero. In this case, equation (23) can be written as

$$W^{(6)}(x) + \left(\frac{\bar{m}\omega^2}{G_sA_s} - \frac{112G_c}{5E_cb^2}\right)W^{(4)}(x) - \left(\frac{8\bar{m}\omega^2}{E_cI} + \frac{112\bar{m}\omega^2G_c}{5G_sA_sE_cb^2}\right)W^{(2)}(x) + \frac{112\bar{m}\omega^2G_c}{5E_c^2b^2I}W(x) = 0 \quad (24)$$

Equation (24) can be solved by first solving the following characteristic equation

$$\lambda^6 + \left(\frac{\bar{m}\omega^2}{G_sA_s} - \frac{112G_c}{5E_cb^2}\right)\lambda^4 - \left(\frac{8\bar{m}\omega^2}{E_cI} + \frac{112\bar{m}\omega^2G_c}{5G_sA_sE_cb^2}\right)\lambda^2 + \frac{112\bar{m}\omega^2G_c}{5E_c^2b^2I} = 0 \quad (25)$$

From the relationship of roots and coefficients in equation (25), one can easily prove that the third-order equation about the variable λ^2 has one negative root (i.e. $\lambda_1^2 < 0$) and another two positive roots (i.e. $\lambda_2^2 > 0$ and $\lambda_3^2 > 0$). Therefore, the six roots of equation (25) are $\pm i\lambda_1$, $\pm\lambda_2$, and $\pm\lambda_3$, respectively. The general solution to equation (24) is

$$W(x) = C_1\cos\lambda_1x + C_2\sin\lambda_1x + C_3\cosh\lambda_2x + C_4\sinh\lambda_2x + C_5\cosh\lambda_3x + C_6\sinh\lambda_3x \quad (26)$$

where $C_i (i = 1-6)$ are the constants which can be determined from the boundary conditions at the two ends of the box girder with CSWs.

Subsection simultaneous method

A two-span continuous box girder with CSWs, as shown in Figure 6, was used as an example to verify the accuracy of the developed formulas for the vertical bending frequencies. The vertical displacement of the first span $W_1(x)$ and that of the second span $W_2(x)$ can be written as

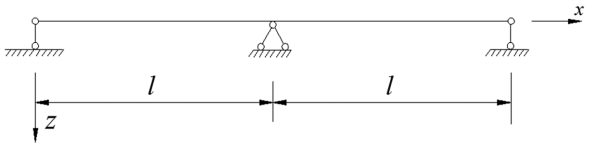

Figure 6. The geometry and boundary condition of a two-span continuous box girder with corrugated steel webs.

$$W_1(x) = A_1\cos\lambda_1x + B_1\sin\lambda_1x + C_1\cosh\lambda_2x + D_1\sinh\lambda_2x + E_1\cosh\lambda_3x + F_1\sinh\lambda_3x \quad (27)$$

$$W_2(x) = A_2\cos\lambda_1x + B_2\sin\lambda_1x + C_2\cosh\lambda_2x + D_2\sinh\lambda_2x + E_2\cosh\lambda_3x + F_2\sinh\lambda_3x \quad (28)$$

where $A_i, B_i, C_i, D_i, E_i, F_i$ $(i = 1, 2)$ are the constants which can be determined from the boundary conditions at the two ends of the box girder with CSWs.

The angular rotation of the cross-section about the y-axis $\varphi_1'(x)$ of the first span and $\varphi_2'(x)$ of the second span can be written as

$$\begin{aligned}\varphi'_1(x) = {} & A_1\left(\frac{\bar{m}\omega^2}{G_sA_s} - \lambda_1^2\right)\cos\lambda_1x + B_1\left(\frac{\bar{m}\omega^2}{G_sA_s} - \lambda_1^2\right)\sin\lambda_1x \\ & + C_1\left(\frac{\bar{m}\omega^2}{G_sA_s} + \lambda_2^2\right)\cosh\lambda_2x + D_1\left(\frac{\bar{m}\omega^2}{G_sA_s} + \lambda_2^2\right)\sinh\lambda_2x \\ & + E_1\left(\frac{\bar{m}\omega^2}{G_sA_s} + \lambda_3^2\right)\cosh\lambda_3x + F_1\left(\frac{\bar{m}\omega^2}{G_sA_s} + \lambda_3^2\right)\sinh\lambda_3x\end{aligned} \quad (29)$$

$$\begin{aligned}\varphi'_2(x) = {} & A_2\left(\frac{\bar{m}\omega^2}{G_sA_s} - \lambda_1^2\right)\cos\lambda_1x + B_2\left(\frac{\bar{m}\omega^2}{G_sA_s} - \lambda_1^2\right)\sin\lambda_1x \\ & + C_2\left(\frac{\bar{m}\omega^2}{G_sA_s} + \lambda_2^2\right)\cosh\lambda_2x + D_2\left(\frac{\bar{m}\omega^2}{G_sA_s} + \lambda_2^2\right)\sinh\lambda_2x \\ & + E_2\left(\frac{\bar{m}\omega^2}{G_sA_s} + \lambda_3^2\right)\cosh\lambda_3x + F_2\left(\frac{\bar{m}\omega^2}{G_sA_s} + \lambda_3^2\right)\sinh\lambda_3x\end{aligned} \quad (30)$$

The additional maximum angular rotation of the flange sections of the box girder of the first span $\xi_1(x)$ and that of the second span $\xi_2(x)$ can be written as

$$\xi_1(x) = -\frac{4}{3E_cI}\left(A_1\frac{E_cI\lambda_1^4-\bar{m}\omega^2\left(\frac{E_cI\lambda_1^2}{G_sA_s}-1\right)}{-\lambda_1^3}\sin\lambda_1 x + B_1\frac{E_cI\lambda_1^4-\bar{m}\omega^2\left(\frac{E_cI\lambda_1^2}{G_sA_s}-1\right)}{\lambda_1^3}\cos\lambda_1 x + C_1\frac{E_cI\lambda_2^4+\bar{m}\omega^2\left(\frac{E_cI\lambda_2^2}{G_sA_s}+1\right)}{\lambda_2^3}\sinh\lambda_2 x + D_1\frac{E_cI\lambda_2^4+\bar{m}\omega^2\left(\frac{E_cI\lambda_2^2}{G_sA_s}+1\right)}{\lambda_2^3}\cosh\lambda_2 x + E_1\frac{E_cI\lambda_3^4+\bar{m}\omega^2\left(\frac{E_cI\lambda_3^2}{G_sA_s}+1\right)}{\lambda_3^3}\sinh\lambda_3 x + F_1\frac{E_cI\lambda_3^4+\bar{m}\omega^2\left(\frac{E_cI\lambda_3^2}{G_sA_s}+1\right)}{\lambda_3^3}\cosh\lambda_3 x\right) \tag{31}$$

$$\xi_2(x) = -\frac{4}{3E_cI}\left(A_2\frac{E_cI\lambda_1^4-\bar{m}\omega^2\left(\frac{E_cI\lambda_1^2}{G_sA_s}-1\right)}{-\lambda_1^3}\sin\lambda_1 x + B_2\frac{E_cI\lambda_1^4-\bar{m}\omega^2\left(\frac{E_cI\lambda_1^2}{G_sA_s}-1\right)}{\lambda_1^3}\cos\lambda_1 x + C_2\frac{E_cI\lambda_2^4+\bar{m}\omega^2\left(\frac{E_cI\lambda_2^2}{G_sA_s}+1\right)}{\lambda_2^3}\sinh\lambda_2 x + D_2\frac{E_cI\lambda_2^4+\bar{m}\omega^2\left(\frac{E_cI\lambda_2^2}{G_sA_s}+1\right)}{\lambda_2^3}\cosh\lambda_2 x + E_2\frac{E_cI\lambda_3^4+\bar{m}\omega^2\left(\frac{E_cI\lambda_3^2}{G_sA_s}+1\right)}{\lambda_3^3}\sinh\lambda_3 x + F_2\frac{E_cI\lambda_3^4+\bar{m}\omega^2\left(\frac{E_cI\lambda_3^2}{G_sA_s}+1\right)}{\lambda_3^3}\cosh\lambda_3 x\right) \tag{32}$$

The boundary conditions for the anti-symmetric mode shapes of two-span continuous box girders with CSWs can be written as follows: $W_1(0) = 0$, $W_1(l) = 0$, $W_2(0) = 0$, $W_2(l) = 0$, $\varphi_1'(0) = 0$, $\varphi_2'(l) = 0$, $\varphi_1'(l) = \varphi_2'(0) = 0$, $\varphi_1(l) = \varphi_2(0)$, $\xi_1'(0) = 0$, $\xi_2'(l) = 0$, $\xi_1'(l) = \xi_2'(0)$, and $\xi_1(l) = \xi_2(0)$. These equations can be satisfied only when the following equations hold:

$$\sin(\lambda_1 l) = 0 \tag{33}$$

$$\lambda_1 = \frac{n\pi}{l} \tag{34}$$

Substituting equation (34) into equation (25), the natural frequencies of the anti-symmetric modes of the girder can be obtained as

$$\omega_f = a_f\sqrt{\frac{E_cI}{\bar{m}}}\left(\frac{n\pi}{l}\right)^2 \tag{35}$$

$$a_f = \frac{\sqrt{1+\frac{5E_cb^2}{112G_c}\left(\frac{n\pi}{l}\right)^2}}{\sqrt{1+\frac{E_cI}{G_sA_s}\left(\frac{n\pi}{l}\right)^2+\frac{5E_cb^2}{14G_c}\left(\frac{n\pi}{l}\right)^2+\frac{5E_c^2b^2I}{112G_cG_sA_s}\left(\frac{n\pi}{l}\right)^4}} \tag{36}$$

The boundary conditions for symmetric mode shapes of two-span continuous box girders with CSWs can be written as follows: $W_1(0) = 0$, $W_1(l) = 0$, $W_2(0) = 0$, $W_2(l) = 0$, $\varphi_1'(0) = 0$, $\varphi_2'(l) = 0$, $\varphi_1'(l) = \varphi_2'(0)$, $\varphi_1(l) = \varphi_2(0) = 0$, $\xi_1'(0) = 0$, $\xi_2'(l) = 0$, $\xi_1'(l) = \xi_2'(0)$, and $\xi_1(l) = \xi_2(0)$. These equations can be satisfied only when the following relationship holds

$$\lambda_1 = \frac{1+4n}{4l}\pi \tag{37}$$

Substituting equation (37) into equation (25), the natural frequencies of the symmetric modes of the girder can be obtained as

$$\omega_z = a_z\sqrt{\frac{E_cI}{\bar{m}}}\left(\frac{1+4n}{4l}\pi\right)^2 \tag{38}$$

$$a_z = \frac{\sqrt{1+\frac{5E_cb^2}{112G_c}\left(\frac{1+4n}{4l}\pi\right)^2}}{\sqrt{1+\frac{E_cI}{G_sA_s}\left(\frac{1+4n}{4l}\pi\right)^2+\frac{5E_cb^2}{14G_c}\left(\frac{1+4n}{4l}\pi\right)^2+\frac{5E_c^2b^2I}{112G_cG_sA_s}\left(\frac{1+4n}{4l}\pi\right)^4}} \tag{39}$$

From the expressions of a_f and a_z, it can be seen that the shear deformation effect of CSWs is included in the second term in the denominator, while the effect of shear lag of the box girder is included in the second term in the numerator and the third term in the denominator. The coupling effect considering the shear lag and shear deformation of CSWs is included in the fourth term of the denominator. As for the existing formulas for calculating the vibration frequencies of girder bridges, none of these effects is considered.

Comparing the anti-symmetric and symmetric vibration modes of two-span continuous box girders with CSWs, it can be seen that the frequencies of the anti-symmetric modes are composed of odd-numbered frequencies, that is, the first, third, fifth frequencies, and so on, while the frequencies of the symmetric modes are composed of even-numbered frequencies, that is, the second, fourth, sixth frequencies, and so on.

Experimental study

Bridge model and test setup

The bridge model used in the experimental study is a one-tenth scale model built for the Juancheng Yellow River Bridge located in Shandong Province, China. This bridge model is a two-span continuous concrete box-girder bridge with CSWs. The length of the bridge model is 6 m in total. The CSWs of the bridge model have a thickness of 1.2 mm. The steel material has a

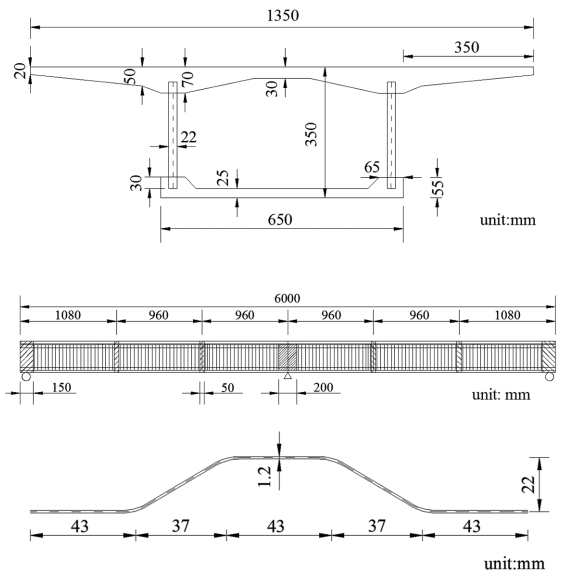

Figure 7. Dimensions of the PC box-girder bridge model with CSWs: (a) cross-sectional view, (b) elevation view, and (c) corrugated steel web.

yielding stress of f_y = 296 MPa, Poisson's ratio of v_s = 0.3, and Young's modulus of E_s = 206 GPa. The compressive strength f_c, Young's modulus E_c, and Poisson's ratio v_c for the upper and lower concrete flanges are taken as 51.2 MPa, 34.5 GPa, and 0.2, respectively. The dimensions of the PC box-girder bridge model with CSWs are shown in Figure 7.

For the boundary condition, the bridge model is supported by a hinge in the middle and a roller support at each end. Two prestressing tendons were used in the bridge model, as shown in Figure 8, with the prestressing force monitored by the pressure sensors installed at the two ends of the bridge model. An effective prestressing force of 130 kN was applied on each prestressing tendon.

Modal test

Modal test was performed to obtain the natural frequencies and mode shapes of the bridge model. A total of 11 measurement points were selected on the bridge deck, as shown in Figure 9.

Both vertical and lateral accelerations were recorded at each measurement point and the sampling rate was set to 512 Hz. An impact hammer was used to excite the vibration of the bridge model. A sample of the measured vertical acceleration time history at Point 3 is plotted in Figure 10. The collected data were then processed using commercial software and the first two natural frequencies obtained were 61.94 and 75.94 Hz, respectively. The corresponding mode shapes of the first two modes are provided in Figure 11. It should be noted that the modal information of higher modes was not obtained due to the difficulty associated with exciting higher modes in the modal test.

Results and discussion

The results obtained from both the experimental study and FE analysis (using the MIDAS software) were

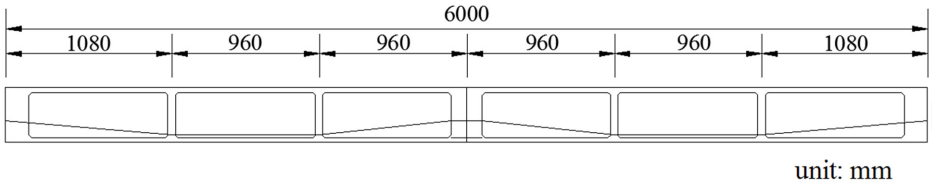

Figure 8. Layout of the prestressing tendons.

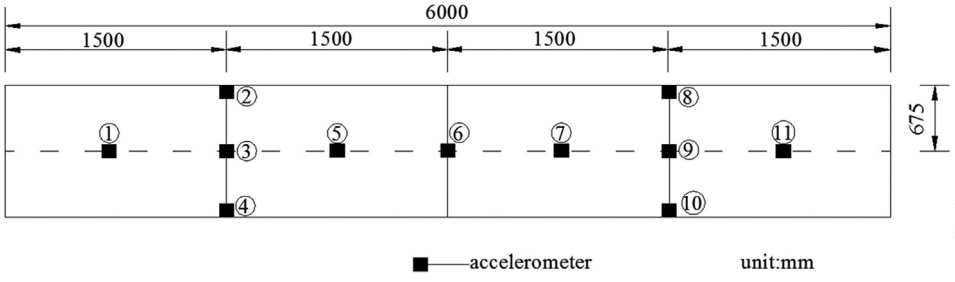

Figure 9. Measurement locations on the bridge deck in the modal test (unit: mm).

Table 2. Comparison of modal test results.

Mode number	Proposed formulas in this article		FE analysis results		Modal test results	
	Frequency (Hz)	Type of mode	Frequency (Hz)	Type of mode	Frequency (Hz)	Type of mode
1	54.74	VAF	55.65	VAF	61.94	VAF
2	73.98	VSF	75.41	VSF	75.94	VSF
3	131.03	VAF	134.10	VAF	–	–
4	149.72	VSF	153.30	VSF	–	–
5	205.17	VAF	210.08	VAF	–	–
6	223.52	VSF	228.79	VSF	–	–

VAF: vertical anti-symmetric flexural; VSF: vertical symmetric flexural.

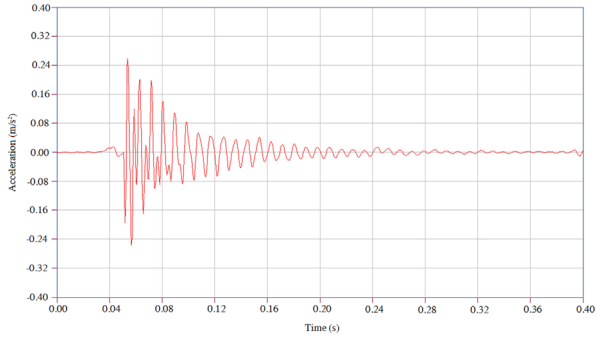

Figure 10. Measured acceleration time history at Point 3.

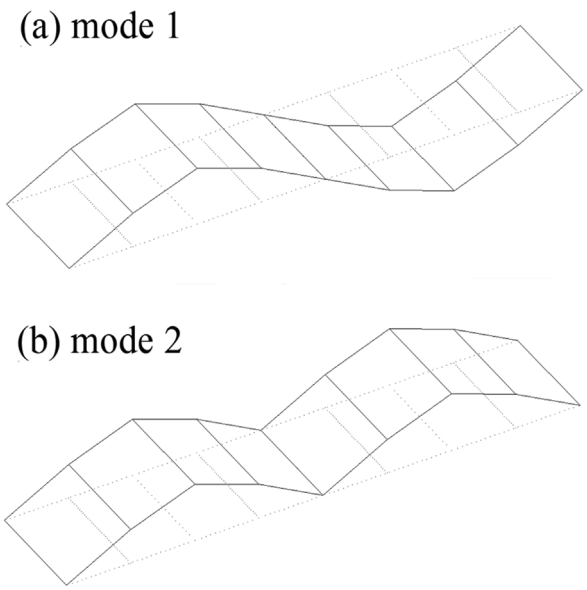

Figure 11. The first two mode shapes obtained from the modal test: (a) mode 1 and (b) mode 2.

used to verify the accuracy of the proposed formulas for the vertical bending vibration frequencies of PC box girders with CSWs, as shown in Table 2. The FE

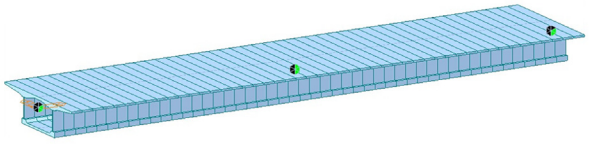

Figure 12. The finite element model of the tested girder model.

model of the PC box girder with CSWs created using the MIDAS software is shown in Figure 12. In this model, the CSWs were modeled using the composite beam elements, the prestressed tendons were modeled by three-dimensional (3D) two-node spar elements. The end supports were constrained in both the vertical and lateral directions while the movements in the vertical, lateral, and longitudinal directions were constrained for the middle support. Based on the modal analysis in MIDAS, the natural frequencies of the model are summarized in Table 2 while the first six mode shapes are shown in Figure 13.

From Table 2, it can be observed that all six natural frequencies as well as the corresponding mode shapes obtained from proposed method agree very well with the results from the FE analysis. The second frequency obtained from the modal test on the bridge model also agrees with both the calculated frequency using the proposed formula and the FE analysis result very well; however, the fundamental natural frequency of the bridge model from the modal test is about 10% greater than the other two results. This could be due to the fact that the hinge at the middle of the girder is not perfectly smooth and therefore restraints the rotation of the girder to some degree and that the measured size of the girder is slightly larger than the designed.

In addition, it can also be observed that the calculated frequencies using the proposed formula are slightly smaller than FE analysis results. This is possibly due to the fact that the MIDAS software only considers the effect of shear deformation of steel webs

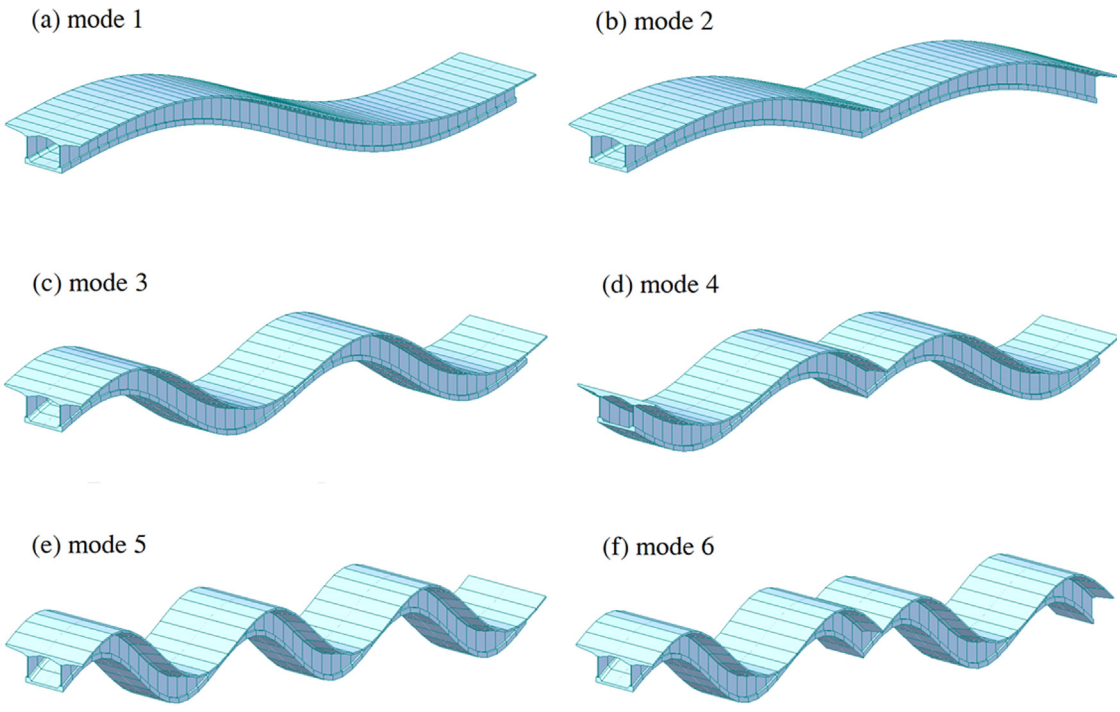

Figure 13. The first six mode shapes of the girder model: (a) mode 1, (b) mode 2, (c) mode 3, (d) mode 4, (e) mode 5, and (f) mode 6.

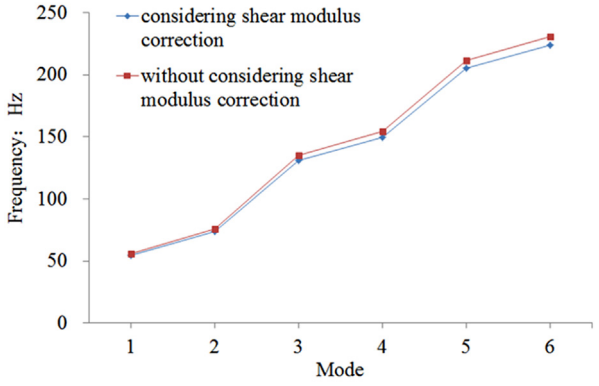

Figure 14. The vertical bending vibration frequencies with and without considering the shear modulus correction.

while ignoring the shear-lag effect and the coupling effect.

The effect of shear modulus correction on the vibration of the bridge model was also investigated. The first six vertical bending vibration frequencies of the bridge model with CSWs, with and without considering the effect of shear modulus correction, were obtained using the proposed method in this article, and the results are shown in Figure 14.

As can be seen from Figure 14, small differences are observed between the vibration frequencies of the girder with and without considering the effect of shear modulus correction of the CSWs.

The effect of different beam theories on the vibration of the girder was also investigated. The Euler–Bernoulli beam theory and Timoshenko beam theory were studied. The vertical bending vibration frequencies of the bridge model by adopting the Euler–Bernoulli beam theory and Timoshenko beam theory were obtained and compared to the results predicted by the proposed method in this study, as shown in Figure 15.

It can be seen from Figure 15 that the frequencies predicted by the proposed method in this study agree very well with those calculated according to the Timoshenko beam theory while both are significantly smaller than the results obtained using the Euler–Bernoulli beam theory. Since the Timoshenko beam theory only considers the shear deformation of the CSWs, these observations indicate that the shear deformation of the CSWs has a significant influence on the vertical bending vibration frequencies of the bridge model with CSWs, while the shear-lag effect and the coupling effect have little influence on the vertical bending vibration frequencies of bridge model with CSWs.

Table 3. The first six vertical bending vibration frequencies of bridge models with different span lengths.

Mode number	Span-to-length ratio									
	0.108		0.130		0.163		0.217		0.325	
	Proposed method (Hz)	T-beam theory (Hz)	Proposed method (Hz)	T-beam theory (Hz)	Proposed method (Hz)	T-beam theory (Hz)	Proposed method (Hz)	T-beam theory (Hz)	Proposed method (Hz)	T-beam theory (Hz)
1	18.44	18.59	25.10	25.36	35.85	36.33	54.74	55.71	93.17	95.27
2	26.84	27.13	35.85	36.33	49.96	50.80	73.98	75.51	121.63	124.58
3	54.74	55.71	70.13	71.54	93.17	95.27	131.03	134.26	205.17	210.38
4	64.36	65.60	81.67	83.43	107.45	109.98	149.72	153.48	232.67	238.51
5	93.17	95.27	115.97	118.75	149.72	153.48	205.17	210.38	314.77	322.18
6	102.70	105.09	127.27	130.39	163.66	167.81	223.52	229.15	342.09	349.90

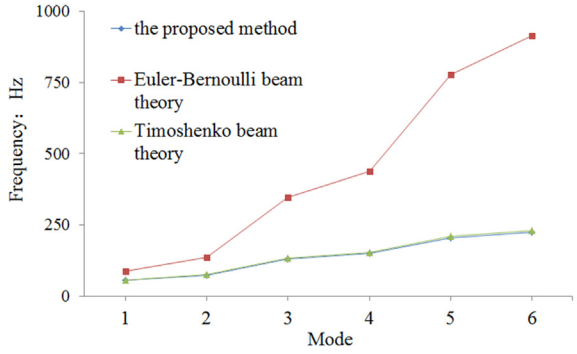

Figure 15. Comparison of vertical bending frequencies obtained by different methods.

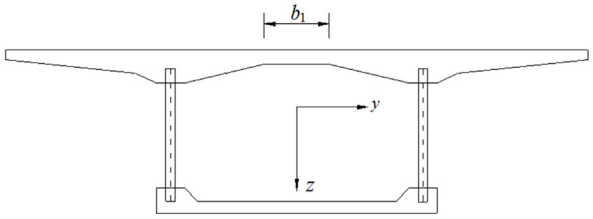

Figure 16. Geometric shape of flat section.

Parametric study

In order to further evaluate the proposed formulas, a parametric study was conducted to investigate the effect of two important parameters, namely the width-to-span ratio and corrugation pattern, on the vibration of the girder with CSWs. The results obtained from the proposed formulas are compared to those obtained using other methods.

Effect of width-to-span ratio

The effect of the width-to-span ratio on the vertical bending vibration of the girder was studied through first changing the span length of the bridge model with CSWs. In order to make a fair comparison, the height of the bridge model was assumed as constant. Five bridge span lengths were investigated, namely, 2, 3, 4, 5, and 6 m for each span of the continuous bridge, respectively, which correspond to width-to-span ratios of 0.325, 0.217, 0.163, 0.130, and 0.108. The first six vertical bending vibration frequencies were obtained for these bridge models, as summarized in Table 3, where these results are compared to the results obtained using the Timoshenko beam theory (T-beam theory).

As can be seen from Table 3, for all different span lengths studied, the vertical bending vibration frequencies of the bridge model with CSWs obtained from the proposed method in this article and the Timoshenko beam theory are in good agreement. Therefore, the vertical bending vibration frequencies of bridge model with CSWs can be predicted using the Timoshenko beam theory in practice. In addition, it can also be observed that the calculated frequencies using the proposed formula are slightly smaller than the results obtained using the Timoshenko beam theory. This could be due to the fact that the Timoshenko beam theory only considers the effect of the shear deformation of the steel webs without considering the shear-lag effect and the coupling effect.

The effect of width-to-span ratio was also studied by varying the width of the girder while assuming constant girder height and span length. Different values of the width of the flat section, as denoted by b_1 in Figure 16, are assumed, namely, $0.5b_1$, $1.5b_1$, $2.5b_1$, $3.5b_1$, respectively. These values correspond to width-to-span ratios of 0.192, 0.242, 0.292, and 0.342, respectively. The vertical bending vibration frequencies with the different girder widths were obtained and the first six modes are summarized in Table 4.

Table 4. The first six vertical bending vibration frequencies of bridge models with different girder widths.

Mode number	Span-to-length ratio							
	0.192		0.242		0.292		0.342	
	Proposed method (Hz)	T-beam theory (Hz)	Proposed method (Hz)	T-beam theory (Hz)	Proposed method (Hz)	T-beam theory (Hz)	Proposed method (Hz)	T-beam theory (Hz)
1	55.48	56.49	54.28	55.19	53.10	53.94	52.38	53.12
2	75.18	76.79	73.09	74.52	71.65	72.93	69.68	70.80
3	133.73	137.19	128.73	131.70	124.24	126.84	120.51	122.71
4	152.93	156.96	146.96	150.41	141.64	144.64	137.16	139.69
5	209.85	215.46	201.03	205.79	193.27	197.37	186.61	190.04
6	228.68	234.76	218.93	224.07	210.36	214.79	202.99	206.68

Table 5. The first six vertical bending vibration frequencies under different corrugation wave patterns.

Mode number	Frequency (Hz)		
	CW1	CW2	CW3
1	54.74	54.35	53.94
2	73.98	73.42	72.72
3	131.03	129.81	128.31
4	149.72	148.29	146.52
5	205.17	203.10	200.54
6	223.52	221.24	218.42

It can be seen from Table 4 that the vertical bending vibration frequencies of the bridge model with CSWs obtained from the proposed formulas agree well with the results from using the Timoshenko beam theory despite the varying width-to-span ratios due to the change of girder width.

Effect of corrugation pattern

Assuming the same web height and thickness, the effect of corrugation pattern on the vertical bending vibration frequencies of the bridge model with CSWs was studied. Three types of corrugation wave patterns, namely CW1, CW2, and CW3 with parameters provided in Table 1, were considered. The results for these three corrugation wave patterns are shown in Table 5.

It can be seen from Table 5 that the difference of vertical bending vibration frequencies of the bridge model with CSWs caused by different corrugation wave patterns is very small.

Comparison with the Chinese code and other research results

The fundamental natural frequency is one of the most important dynamic characteristics of bridges and it plays a very important role in predicting the dynamic performance of the bridge structure under external loads, such as wind, earthquake, and moving vehicles. To the best knowledge of the authors, no bridge design code has yet provided any simple formula for calculating the natural frequencies of continuous PC girders with CSWs. Therefore, the best references available would be some bridge design codes or existing research results which provide such formulas for predicting the natural frequencies for continuous PC girders although such information is also very limited in the literature.

The current Chinese General Code for Design of Highway Bridges and Culverts (MCPRC, 2004) defines the dynamic impact factor as a function of the bridge fundamental frequency and provides the following formulas for estimating the fundamental frequency of continuous bridges

$$f_{11} = \frac{13.616}{2\pi l^2}\sqrt{\frac{EI_c}{m_c}} \tag{40}$$

$$f_{12} = \frac{23.651}{2\pi l^2}\sqrt{\frac{EI_c}{m_c}} \tag{41}$$

where E is Young's modulus of the material, I_c is the moment of inertia of the structure cross-section, m_c is the mass per unit length of the structure cross-section, and l is the span length. It is stated in the code that f_{11} should be used when calculating the impact factor for positive bending moment and shear, while f_{12} should be used when calculating the impact factor for negative bending moment.

Gao et al. (2012) proposed an improved method to estimate the fundamental frequency of continuous girder bridges and verified the accuracy of the proposed method by theoretical analysis combined with numerical simulations. In their study, the following expression was proposed for estimating the natural frequencies of two-span continuous girder bridges with uniform cross-section and uniform spans

$$f_n = \frac{1}{2\pi l^2}(\pi^2, 3.927^2, 4\pi^2, \ldots)\left(\sqrt{\frac{EI_c}{m_c}}\right)^2 \quad (42)$$

The fundamental frequency of the scale bridge model predicted by equations (40) to (42) is 118.99, 206.69, and 86.25 Hz, respectively, while the value calculated using the proposed formula in this study is 54.74 Hz, indicating that the fundamental frequency obtained from the Chinese design code and Gao et al. (2012) is significantly larger than the frequency predicted by the proposed method in this study. These large differences clearly indicate the need for proposing specific formulas for accurately predicting the natural frequencies of PC box-girder bridges with CSWs.

Summary and conclusion

In this study, formulas for predicting the vertical bending vibration frequencies of PC box girders with CSWs were proposed based on Hamilton's energy variational principle. To verify the accuracy of the formulas, a one-tenth scale model was developed for an existing PC box-girder bridge with CSWs. The results predicted from the proposed formulas were compared to the results obtained from the FE analysis and also the experimental results from the scale bridge model. Good agreement was achieved between these results, indicating that the proposed formulas can provide a reliable and efficient tool to predict the vertical bending vibration frequencies of the PC box-girder bridges with CSWs. Based on the results from the parametric study, the following conclusions can also be drawn:

1. The proposed method can be adopted in the analysis of a full girder bridge with confidence and can significantly reduce the modeling effort and computational effort in the FE analysis. The results obtained from the proposed method are more accurate than those obtained using theoretical methods.
2. The effect of shear deformation of the CSWs on the vertical bending vibration frequencies of bridges with CSWs is significant, while the shear-lag effect and the coupling effect between the shear lag and shear deformation have negligible influence on the vertical bending vibration frequencies of bridge with CSWs. In addition, the difference between the results with and without considering the shear modulus correction is very small.
3. The vertical bending vibration frequencies of bridges with CSWs predicted by the proposed formulas agree well with those calculated based on the Timoshenko beam theory for a wide range of width-to-span ratios considered.
4. The corrugation wave patterns considered in this study have little effect on the vertical bending vibration frequencies of bridges with CSWs.
5. The existing formulas for predicting the fundamental vibration frequency of continuous bridges provided in the Chinese design code (JTG D60-2004) and the available research results may significantly overestimate the fundamental frequency of PC continuous box-girder bridges with CSWs and should be used with caution.

It should be noted that the method proposed in this study is applicable for analyzing the global responses of PC box-girder bridges with CSWs, including the modal responses and global displacements. It is not suitable for the analysis of local responses such as local displacements and strains.

Declaration of Conflicting Interests

The author(s) declared no potential conflicts of interest with respect to the research, authorship, and/or publication of this article.

Funding

The author(s) disclosed receipt of the following financial support for the research, authorship, and/or publication of this article: The work described in this article was supported partially by two grants from the National Natural Science Foundation of China (Grant No. 51368032 and Grant No. 51208189) and partially by a grant from the Postdoctoral Science Foundation of China (2014M562103).

References

Abbas HH, Sause R and Driver RG (2007a) Analysis of flange transverse bending of corrugated web I-girders under in-plane loads. *Journal of Structural Engineering: ASCE* 133(3): 347–355.

Abbas HH, Sause R and Driver RG (2007b) Simplified analysis of flange transverse bending of corrugated web I-girders under in-plane moment and shear. *Engineering Structures* 29: 2816–2824.

Bertagnoli G, Biagini MA and Mancini G (2012) Orthotropic model for the analysis of beams with corrugated steel webs. In: Fardis MN (ed.) *Innovative Materials and Techniques in Concrete Construction*, vol. 24. Dordrecht: Springer, pp. 361–375.

Driver RG, Abbas HH and Sause R (2006) Shear behavior of corrugated web bridge girder. *Journal of Structural Engineering: ASCE* 132(2): 195–203.

Easley JT and McFarland DE (1969) Buckling of light-gage corrugated metal shear diaphragms. *Journal of Structural Division* 95(7): 1497–1516.

Elgaaly M, Hamilton RW and Seshadri A (1996) Shear strength of beams with corrugated webs. *Journal of Structural Engineering: ASCE* 122(4): 390–398.

Elgaaly M, Seshadri A and Hamilton RW (1997) Bending strength of steel beams with corrugated webs. *Journal of Structural Engineering: ASCE* 123(6): 772–782.

Gao Q, Wang Z, Liu Y, et al. (2012) Modified formula of estimating fundamental frequency of girder bridge with uniform cross-section. *Advanced Engineering Forum* 5: 177–182.

Hassanein MF and Kharoob OF (2014) Shear buckling behavior of tapered bridge girders with steel corrugated webs. *Engineering Structures* 74: 157–169.

Huang L, Hikosaka H and Komine K (2004) Simulation of accordion effect in corrugated steel web with concrete flanges. *Computers & Structures* 82: 2061–2069.

Ibrahim SA (2001) *Fatigue analysis and instability problems of plate girders with corrugated webs*. PhD Dissertation, Drexel University, Philadelphia, PA.

Ji W, Liu S and Lin P (2012) Dynamic analysis of a continuous box girder with corrugated steel webs. *Journal of Highway and Transportation Research and Development* 6(4): 78–82.

Luo Q, Tang J and Li Q (2004) Shear lag analysis of beam-columns. *Engineering Structures* 26: 2113–2124.

Ministry of Communication of the People's Republic of China (MCPRC) (2004) *JTG D60-2004 General Code for Design of Highway Bridges and Culverts*. Beijing, China: MCPRC.

Mo YL, Jeng CH and Chang YS (2000) Torsional behavior of prestressed concrete box-girder bridges with corrugated steel webs. *ACI Structural Journal* 97(6): 849–859.

Mo YL, Jeng CH and Krawinkler H (2003) Experimental studies of prestressed concrete box-girder bridges with corrugated steel webs. In: *Proceedings of the international conference on high performance materials in bridges*, Kona, HI, 29 July–3 August, pp. 209–218. Reston, VA: ASCE.

Moghimi H and Ronagh HR (2008) Impact factors for a composite steel bridge using non-linear dynamic simulation. *International Journal of Impact Engineering* 35: 1228–1243.

Moon J, Yi J, Choi BH, et al. (2009) Shear strength and design of trapezoidally corrugated steel webs. *Journal of Constructional Steel Research* 65: 1198–1205.

Nguyen ND, Kim SN, Han SR, et al. (2010) Elastic lateral-torsional buckling strength of I-girder with trapezoidal web corrugations using a new warping constant under uniform moment. *Engineering Structures* 32: 2157–2165.

Ontario Ministry of Transportation and Communications (OMTC) (1983) *Ontario Highway Bridge Design Code (OHBDC)*. Toronto, ON, Canada: OMTC.

Reissner E (1946) Analysis of shear lag in box beams by the principle of minimum potential energy. *Quarterly of Applied Mathematics* 5(3): 268–278.

Samanta A and Mukhopadhyay M (1999) Finite element static and dynamic analyses of folded plates. *Engineering Structures* 21: 277–287.

Sayed-Ahmed EY (2005) Lateral torsion-flexure buckling of corrugated web steel girders. *Proceedings of the Institution of Civil Engineers: Structures and Buildings* 158(1): 53–69.

Wu Y, Liu S, Zhu Y, et al. (2003) Matrix analysis of shear lag and shear deformation in thin-walled box beams. *Journal of Engineering Mechanics: ASCE* 129(8): 944–950.

Yi J, Gil H, Youm K, et al. (2008) Interactive shear buckling behavior of trapezoidally corrugated steel webs. *Engineering Structures* 30: 1659–1666.